Monatshefte für Chemie - Chemical Monthly (2024) 155:313–317
https://doi.org/10.1007/s00706-023-03163-3

ORIGINAL PAPER

Basic method for water detection in $LiPF_6$-based electrolytes

Antonín Šimek[1] · Tomáš Kazda[1] · Jiří Báňa[1] · Ondřej Čech[1]

Received: 29 September 2023 / Accepted: 11 December 2023 / Published online: 24 January 2024

Abstract

This paper investigates the effect of water content on lithium-ion battery electrolytes with particular emphasis on the degradation of lithium hexafluorophosphate, a commonly used salt in commercial electrolytes. The study addresses various degradation mechanisms caused by water in a battery system. In addition, the research utilizes electrochemical techniques to detect water and associated changes in electrochemical performance of the cell. The electrochemical water detection method investigated is very fast. The lower detection limit was not tested, but contamination of 250 ppm can be reliably detected. It can be used, for example, in experimental research to determine the purity and quality of the electrolyte used.

Graphical abstract

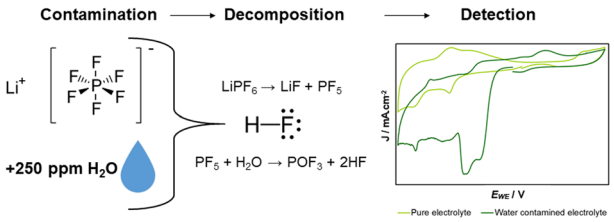

Keywords Lithium-ion batteries · Decomposition · Electrochemistry · Cyclic voltammetry · Corrosion

Introduction

Lithium-ion battery (LIB) technology is one of the most commonly used today. They find their application not only in consumer electronics, but also in stationary energy storage and in the constantly developing electromobility. It is mainly due to their advantageous properties, such as high gravimetric and volumetric energy and power densities, relatively long lifetime, varying size of individual cells, and reliability [1].

Generally, a LIB battery consists of a positive and negative electrode, respective current collectors, a porous separator and an ion-conducting electrolyte. $LoCoO_2$ (LCO), $LiNi_xMn_yCo_{1-x-y}O_2$ (NMC), $LiFePO_4$ (LFP), $LiNi_xCo_yAl_zO_2$ (NCA) and others are commonly used as the positive electrode [2]. Graphite is most commonly used as the negative electrode. The respective current collectors become aluminum for the positive electrode and copper for the negative electrode. The porous separator is most often composed of a polymeric foil, and the electrolyte is then composed of a lithium salt dissolved in a suitable solvent or a mixture of solvents [3].

The role of electrolyte in Li-ion batteries

The electrolyte is an essential part of the Li-ion battery as it ensures the transfer of ions between the anode and cathode. The electrolyte is also involved in the formation of the solid electrolyte interphase (SEI) [4–6] on anode during the initial cycling of the battery. The electrolyte is also involved in the formation of the Cathode Electrolyte Interphase (CEI) [7] at the cathode. These layers ensure compatibility between the electrodes and the electrolyte [8]. The electrolyte is therefore in contact with all the active

✉ Antonín Šimek
Antonin.Simek1@vut.cz

[1] Department of Electrical and Electronic Technology, Faculty of Electrical Engineering and Communication, Brno University of Technology, Brno, Czech Republic

parts of the battery, so it must meet several properties [9]. Key properties include good ionic conductivity to ensure the transfer of Li^+ ions between the anode and cathode; low electron conductivity to prevent internal short circuits, which is aided by the porous separator; and a wide potential window corresponding to the working potentials of the anode and cathode to prevent electrolyte decomposition during battery operation [9–11]. In addition, there is inertness to other parts of the battery to avoid dissolution or corrosion of the current collectors, the battery cover, or the separator; thermal stability over a wide temperature range corresponding to the temperatures in which the battery will be operated; and last but not least, low toxicity of both the electrolyte itself and its manufacturing process [9–11].

Basic electrolyte composition for Li-ion batteries

Electrolytes for Li-ion batteries can be broadly divided into non-aqueous electrolytes consisting of a lithium salt dissolved in an organic solvent; aqueous solutions consisting of a lithium salt that can be dissolved in water; ionic liquids consisting of organic lithium salts; polymer electrolytes; solid electrolytes and hybrid electrolytes [12]. In this work, focus will be given to non-aqueous electrolytes as they are among the most used in modern Li-ion batteries.

Non-aqueous electrolytes for Li-ion batteries consist of a lithium salt dissolved in an organic solvent. Lithium hexafluorophosphate ($LiPF_6$) is the most commonly used lithium salt today, as it provides good operating temperature, great ionic conductivity, large enough potential window and sufficient SEI formation [1]. The use of this salt is to some extent a compromise since, as mentioned in [4], other commercially available salts suffer from several drawbacks that make it disadvantageous to use these salts. For example, lithium hexafluoroarsenate ($LiAsF_6$) is poisonous; lithium perchlorate ($LiClO_4$) is explosive; lithium hexafluoroborate ($LiBF_6$) negatively affects the anode surface; lithium trifluoromethanesulfonate ($LiSO_3CF_3$) has too low ionic conductivity; and lithium bis(trifluoromethanesulfonyl)imide ($LiN(SO_2CF_3)_2$) causes problems with insufficient passivation of the cathode material, leading to corrosion of the aluminum current collector [10].

Organic carbon-based compounds (carbonates) are used as aprotic solvents. The most used include ethylene carbonate (EC), dimethyl carbonate (DMC), diethyl carbonate (DEC) and others. These carbonates are suitable for use as they are stable in 4 V cathode systems and provide stability against surface of lithiated graphite used as anode. Their other properties include a good operating temperature range, high polarity, and low toxicity [11].

Mechanism of $LiPF_6$ based electrolyte decomposition

$LiPF_6$ has relatively high stability in dry inert environments up to 107 °C, but degrades rapidly when exposed to water or moisture. Decomposition process, which can be described by Eq. (1), begins, whereby $LiPF_6$ decomposes to form lithium fluoride (LiF) and phosphorous pentafluoride (PF_5). The PF_5 formed can then react with the water present in the electrolyte to form hydrofluoric acid (HF). This process can be described by Eq. (2) [14]. HF is very corrosive and its presence in the battery system can lead to other degradation processes such as corrosion of the electrodes, corrosion of the current collectors, corrosion of the battery pack, etching of the separator and other undesirable phenomena affecting battery life and performance [14, 15]. These degradation mechanisms are further accompanied by phenomena such as dendritic growth, decrease in capacitance, increase in internal resistance and deterioration in stability and thus safety [16]. It is therefore essential to control the manufacturing process to ensure that no water or moisture enters the battery parts. All parts of the battery must therefore be thoroughly dried during manufacture [17]. However, in commercial LIBs, polyethylene (PE) or polypropylene (PP) film is most commonly used as a separator. According to [18], the presence of HF in the electrolyte deteriorates the stability between the lithium metal and the separator, but lithium metal is not used in commercial LIBs. In general, materials such as PP or PE are resistant to the effects of HF [19].

The $LiPF_6$ decomposition reaction described above is almost negligible at room temperature. However, in an electrolyte environment, interactions between PF_5 and solvent molecules such as EC and DEC occur, shifting the equilibrium of the reaction to the right. This shift results in higher HF formation. The formation of HF is also influenced by the presence of Li^+ ions, as well as by the H^+ protons released during the formation of LiF in SEI at the anode or in CEI at the cathode [13]. This mechanism is described by Eq. (3).

The precipitation of solid LiF(s), and the removal of the Li^+ ion from the solvated system, does not directly affect the formation of HF. However, the released protons can further react with $LiPF_6$ molecules to form more HF [13]. These mechanisms are described by Eq. (4) and (5).

$$LiPF_6 \rightarrow LiF + PF_5, \tag{1}$$

$$PF_5 + H_2O \rightarrow POF_3 + 2HF, \tag{2}$$

$$Li^+ + HF \leftrightarrow LiF(s) + H^+, \tag{3}$$

$$H^+ + PF_6^- \leftrightarrow H - F - PF_5, \tag{4}$$

$$H - F - PF_5 \rightarrow HF + PF_5. \quad (5)$$

The aim of our research is therefore to try to detect the presence of water in electrolytes, which is normally solved using indirect Karl-Fisher titration [14].

Results and discussion

For all material configurations, the light green line plots the cyclic voltammetry (CV) curves for the pure electrolyte. From these curves it is possible to observe the stability of the pure electrolyte during the measurements. The dark green line shows the measured CV curves for the water contaminated electrolyte, whose curves vary depending on the material configuration. In the results for the lithium-steel cell configuration in Fig. 1, a significant cathodic current response can be observed at potentials in the range of 0.05–2.2 V vs. Li/Li^+, which is due to the electrolysis of the water present.

A similar behavior can be observed in the results for the lithium-copper cell configuration shown in Fig. 2, where a strong cathodic current response was measured at a potential in the range 1.5–2.2 V vs. Li/Li^+, again corresponding to electrolysis of the water present.

The results for the lithium-aluminum cell configuration in Fig. 3 then show a anodic current response at a potential of around 4.2 V vs. Li/Li^+ which, according to [20], may be due to the electrochemical response of oxygen produced during the decomposition of $LiPF_6$. Furthermore, it is possible to observe small short-circuits at cathodic potentials around 3.0–3.5 V vs. Li/Li^+, which are caused by the gradual etching of the used glass separator by the HF.

Compared to Karl-Fisher titration, the electrochemical method is significantly faster and less demanding in preparation. However, the level of water contamination cannot be accurately determined, only whether or not the electrolyte is contaminated. For a correct evaluation, however, it is necessary to make a reference measurement on an uncontaminated electrolyte against which the measured results can be compared. Even so, this method appears to be suitable for experimental investigations on other parts of the battery (e.g. anodes or cathodes) to exclude errors in the degraded electrolyte.

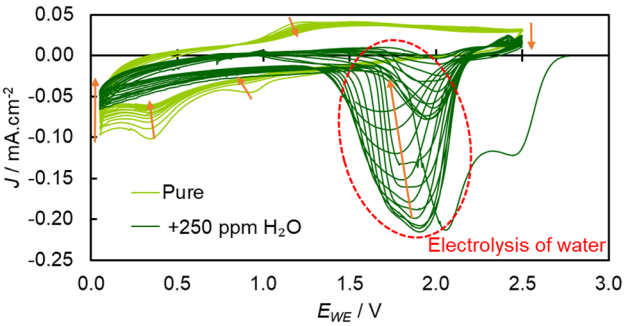

Fig. 2 Measured voltammograms obtained on lithium-copper cell configuration

Effect of HF formation on open-circuit potential curves

The cyclic voltammetry was preceded by an open-circuit potential (E_{OC}) measurement, which served to stabilize the assembled configuration. From these measurements, the effect of HF formation after contamination of the electrolyte with water on these curves was determined. Figure 4 shows the results of the E_{OC} measurements for the lithium-steel cell configuration. First, two reference measurements were made on pure electrolyte, from which an E_{OC} of approximately 1.8 V was obtained. These curves are plotted in light green. Subsequently, measurements were taken with a time delay from water contamination. These intervals were 1.5 h, 54 h, and 96 h from water contamination. From the measured results, it is then possible to observe an increase in E_{OC} up to a value of about 3 V, which is due to the gradual decomposition of $LiPF_6$ described by the Eqs. (1) to (5) in the introduction. On the yellow curve, which was measured 54 h

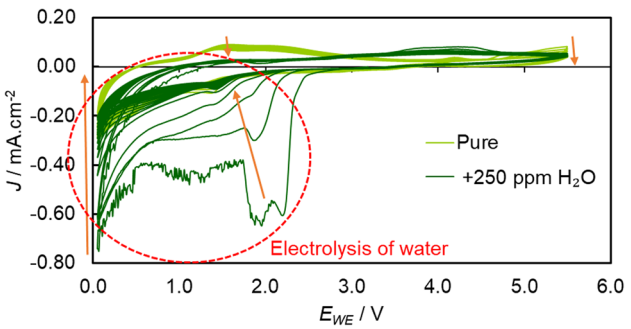

Fig. 1 Measured voltammograms obtained on lithium-steel cell configuration

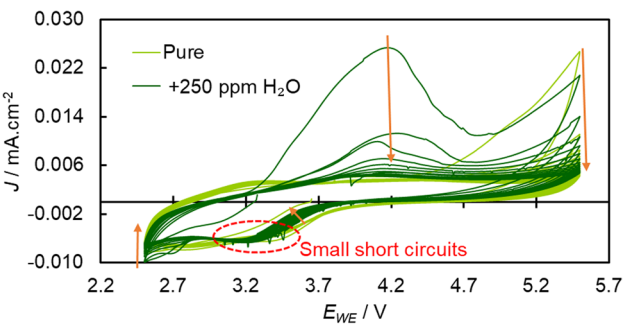

Fig. 3 Measured voltammograms obtained on lithium-aluminum cell configuration

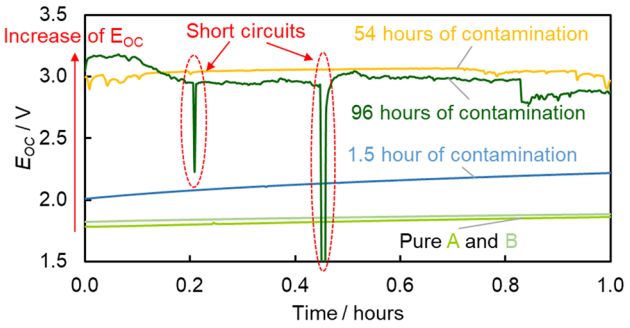

Fig. 4 Influence of HF evolution on open-circuit potential curves

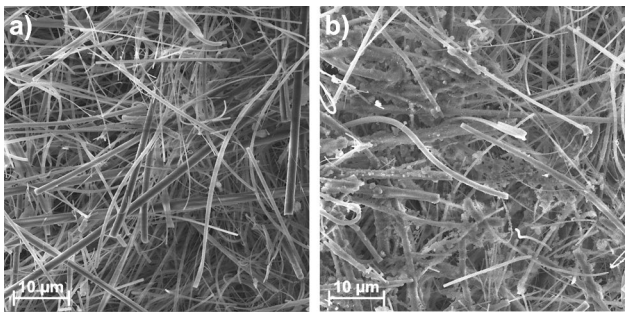

Fig. 5 **a** SEM image of the new glass separator; **b** SEM image of the glass separator used in the measurement 96 h after water contamination

after contamination, an unstable E_{OC} curve can be observed due to the gradual etching of the used glass separator by the HF. On the dark green curve measured 96 h after water contamination, it is then possible to observe a stepwise decrease in E_{OC} caused by a short circuit between the working and counter electrode.

A post-mortem analysis was performed on the Whatman® GF/C glass separator used in the measurements 96 h after water contamination to capture the etched separator. After disassembly of the electrochemical test cell, the separator was dried in an oven at 60 °C (atmospheric pressure) and then transferred to a scanning electron microscope (SEM). An image of the unused glass separator is as reference shown in Fig. 5a. In this image, only pure glass fibers can be observed. From the Energy Dispersive Spectroscopy (EDS) results it was then found that pure glass fibers consist of sodium (Na), silicon (Si), calcium (Ca), aluminum (Al) carbon (C), and oxygen (O).

Figure 5b then shows used glass separator in which a significant difference from the reference can already be observed. For example, the glass fibers are coated with electrolyte residues and other products from the decomposition of $LiPF_6$. From the results of the EDS analysis, fluorine (F), phosphorus (P), and nitrogen (N) were additionally present compared to the original composition of glass fibers. Furthermore, it can be observed that some of the fibers are deformed and glued together, which is most likely due to the etching of the fibers by the HF. In addition, less porosity of the separator can be observed. These phenomena then together deteriorate the insulating ability of the separator, leading to instability and subsequent short circuits.

Conclusion

Commercial lithium-ion batteries typically use a $LiPF_6$-based electrolyte dissolved in carbonate solvents. $LiPF_6$ is very sensitive to water and moisture, which leads to its decomposition and the hydrofluoric acid formation. In our research, we have used fast electrochemical screening methods based on cyclic voltammetry, which are able to detect the presence of water in the electrolyte. Although this method cannot determine the exact concentration of water, it can be used to verify the purity of the electrolyte before using it for further experiments. The method is then faster and less demanding to perform than the Karl-Fisher titration.

Furthermore, the effect of hydrofluoric acid evolution on the E_{OC} curves was determined. The evolving of hydrofluoric acid leads to an increase in E_{OC}, instability and subsequent short circuits. When examining the used glass separator under an electron microscope, deposits formed from the electrolyte itself and probably also products from the decomposition of the lithium salt $LiPF_6$ were observed. Subsequently, minor porosity and minor fiber damage caused by hydrofluoric acid formation resulting in instability and subsequent short circuits were observed on the used separator.

In commercial lithium-ion batteries, this behavior must not occur, and it is therefore essential to control the presence of water and moisture not only in the electrolytes but also in the other parts of battery system during the manufacturing process.

Experimental

In the experimental part, an electrolyte containing lithium salt $LiPF_6$ dissolved in a 1:2 mixture of EC and DMC solvents from SigmaAldrich was used to detect the presence of water. The measurements were first performed on pure electrolyte, then on electrolyte that was contaminated with 250 ppm of H_2O.

To measure the presence of water, electrochemical test cells from EL-CELL® were used in which different material configurations were assembled. All measurements were performed by the three-electrode method. The lithium-steel configuration was used to measure the electrolyte over a full potential range (0.05–5.5 V vs. Li/Li^+); the lithium-copper

configuration was used to measure over a potential window corresponding to the working potential of the anode (0.05–2.5 V vs. Li/Li^+); and the lithium-aluminum configuration was used to measure over a potential window corresponding to the working potential of the cathode (2.5–5.5 V vs. Li/Li^+). Whatman® GF/C glass separator was used in all these configurations.

The electrochemical test cells were assembled in a Jacomex glovebox in the presence of an argon atmosphere (oxygen and water concentrations below 1 ppm). Electrochemical measurements were then performed on a BioLogic VMP-3 multichannel potentiostat. The resulting voltammograms were measured using cyclic voltammetry performed at a scan rate of 5 mV s^{-1}, a total of 20 cycles were performed. The E_{OC} measurements were carried out for one hour, recording the values every 10 s.

A Tescan Lyra 3 SEM equipped with EDS detector was used to take images of the glass separator and to perform elemental analysis.

Acknowledgements This work was supported by the specific graduate research of the Brno University of Technology No. FEKT-S-23-8286. CzechNanoLab project LM2023051 funded by MEYS CR is gratefully acknowledged for the financial support of the measurements at CEITEC Nano Research Infrastructure.

Funding Open access publishing supported by the National Technical Library in Prague.

Data availability The data that support the findings of this study are available from the corresponding author, [Antonín Šimek], upon reasonable request.

References

1. Henschel J, Horsthemke F, Stenzel YP, Evertz M, Girod S, Lürenbaum C, Kösters K, Wiemers-Meyer S, Winter M, Nowak S (2020) J Power Sources 447:227370
2. Rommel SM, Schall N, Brünig C, Weihrich R (2014) Monatsh Chem 145:385
3. Ellis BL, Lee KT, Nazar LF (2010) Chem Mater 22:691
4. Bekaert E, Buannic L, Lassi U, Llordés A, Salminen J (2017) Electrolytes for Li- and Na-ion batteries: concepts, candidates, and the role of nanotechnology. In: Emerging nanotechnologies in rechargeable energy storage systems. Elsevier, p 1
5. Wu Y, Liu X, Wang L, Feng X, Ren D, Li Y, Rui X, Wang Y, Han X, Xu G-L, Wang H, Lu L, He X, Amine K, Ouyang M (2021) Energy Storage Mater 37:77
6. Libich J, Máca J, Vondrák J, Čech O, Sedlaříková M (2017) J Energy Storage 14:383
7. Cech O, Klvac O, Benesova P, Maca J, Cudek P, Vanýsek P (2019) J Energy Storage 22:373
8. Martins VL (2023) Curr Opin Electrochem 38:101241
9. Li Q, Chen J, Fan L, Kong X, Lu Y (2016) Green Energy Environ 1:18
10. Bhattacharyya AJ, Patel M, Das SK (2009) Monatsh Chem 140:1001
11. Logan ER, Tonita EM, Gering KL, Li J, Ma X, Beaulieu LY, Dahn JR (2018) J Electrochem Soc 165:A21
12. Aurbach D, Talyosef Y, Markovsky B, Markevich E, Zinigrad E, Asraf L, Gnanaraj JS, Kim H-J (2004) Electrochim Acta 50:247
13. Lux SF, Lucas IT, Pollak E, Passerini S, Winter M, Kostecki R (2012) Electrochem Commun 14:47
14. Apostolova RD, Shembel EM (2021) Vopr Khim Khim Tekhnol 2021:3
15. Kosfeld M, Westphal B, Kwade A (2022) J Energy Storage 51:104398
16. Cui X, Tang F, Zhang Y, Li C, Zhao D, Zhou F, Li S, Feng H (2018) Electrochim Acta 273:191
17. Chang Z, Qiao Y, Deng H, Yang H, He P, Zhou H (2020) Energy Environ Sci 13:1197
18. Kosfeld M, Westphal B, Kwade A (2023) J Energy Storage 57:106174
19. Li X, Tao J, Hu D, Engelhard MH, Zhao W, Zhang J-G, Xu W (2018) J Mater Chem A 6:5006
20. Sun W, Suo L, Wang F, Eidson N, Yang C, Han F, Ma Z, Gao T, Zhu M, Wang C (2017) Electrochem Commun 82:71